CellPress

Cell Metabolism
Article

The PPARα-FGF21 Hormone Axis Contributes to Metabolic Regulation by the Hepatic JNK Signaling Pathway

Santiago Vernia,[1] Julie Cavanagh-Kyros,[1,2] Luisa Garcia-Haro,[1,8] Guadalupe Sabio,[3] Tamera Barrett,[1,2] Dae Young Jung,[1] Jason K. Kim,[1,4] Jia Xu,[5,9] Hennady P. Shulha,[5] Manuel Garber,[1,6] Guangping Gao,[7] and Roger J. Davis[1,2,*]

[1]Program in Molecular Medicine, University of Massachusetts Medical School, Worcester, MA 01605, USA
[2]Howard Hughes Medical Institute, Worcester, MA 01605, USA
[3]Department of Vascular Biology and Inflammation, Fundación Centro Nacional de Investigaciones Cardiovasculares Carlos III, 28029 Madrid, Spain
[4]Department of Medicine, Division of Endocrinology, Metabolism and Diabetes, University of Massachusetts Medical School, Worcester, MA 01605, USA
[5]Bioinformatics Core, University of Massachusetts Medical School, Worcester, MA 01605, USA
[6]Program in Bioinformatics, University of Massachusetts Medical School, Worcester, MA 01605, USA
[7]Gene Therapy Center, University of Massachusetts Medical School, Worcester, MA 01605, USA
[8]Present address: Department of Cancer Biology, Dana Farber Cancer Institute, Boston, MA 02215, USA
[9]Present address: KEW Group, 790 Memorial Drive, Suite 101, Cambridge, MA 02139, USA
*Correspondence: roger.davis@umassmed.edu
http://dx.doi.org/10.1016/j.cmet.2014.06.010

SUMMARY

The cJun NH_2-terminal kinase (JNK) stress signaling pathway is implicated in the metabolic response to the consumption of a high-fat diet, including the development of obesity and insulin resistance. These metabolic adaptations involve altered liver function. Here, we demonstrate that hepatic JNK potently represses the nuclear hormone receptor peroxisome proliferator-activated receptor α (PPARα). Therefore, JNK causes decreased expression of PPARα target genes that increase fatty acid oxidation and ketogenesis and promote the development of insulin resistance. We show that the PPARα target gene *fibroblast growth factor 21* (*Fgf21*) plays a key role in this response because disruption of the hepatic PPARα-FGF21 hormone axis suppresses the metabolic effects of JNK deficiency. This analysis identifies the hepatokine FGF21 as a critical mediator of JNK signaling in the liver.

INTRODUCTION

The cJun NH_2-terminal kinase (JNK) signaling pathway plays an important role in the development of obesity and insulin resistance (Sabio and Davis, 2010). Indeed, JNK1 deficiency in mice prevents the obesity and insulin resistance caused by hyperphagia or the consumption of a high-fat diet (HFD) (Hirosumi et al., 2002). Studies of tissue-specific JNK-deficient mice demonstrate that these obesity and insulin resistance phenotypes can be separated. Thus, JNK regulation of the hypothalamic-pituitary hormone axis that regulates energy expenditure is critically required for the development of diet-induced obesity (Belgardt et al., 2010; Sabio et al., 2010a; Vernia et al., 2013). In contrast, JNK function in peripheral tissues, including fat, muscle, and inflammatory cells, contributes to diet-induced insulin resistance (Sabio et al., 2008, 2010b; Han et al., 2013).

Consuming a HFD increases the blood concentration of free fatty acids (Kahn et al., 2006) and causes JNK activation mediated by the mixed-lineage protein kinase pathway (Jaeschke and Davis, 2007; Kant et al., 2013). Activated JNK contributes to obesity development by increasing activating protein 1 (AP1)-dependent *Dio2* gene expression in the anterior pituitary gland (Vernia et al., 2013). In contrast, targets of JNK signaling that cause insulin resistance are unclear. Early studies suggested that phosphorylation of the insulin receptor adaptor protein IRS1 by JNK causes insulin resistance (Aguirre et al., 2000), but subsequent studies have not confirmed this conclusion (Copps et al., 2010). More recently, JNK-mediated regulation of adipokines (Sabio et al., 2008) and inflammatory cytokines (Han et al., 2013) has been implicated in the development of insulin resistance. For example, the promotion of hepatic insulin sensitivity caused by JNK deficiency in adipocytes and myeloid cells is associated with defects in adipokine and cytokine expression (Sabio et al., 2008; Han et al., 2013). These data indicate that JNK-mediated hepatic insulin resistance may be caused by JNK function in nonhepatic cells (Sabio et al., 2008; Han et al., 2013). This conclusion is consistent with the finding that whole-body JNK1 deficiency (Hirosumi et al., 2002), but not hepatic JNK1 deficiency (Sabio et al., 2009), protects against HFD-induced insulin resistance. Therefore, the function of hepatic JNK is unclear.

The purpose of this study was to re-evaluate the role of hepatic JNK in the metabolic stress response caused by the consumption of a HFD. It is established that JNK is encoded by the *Jnk1* and *Jnk2* genes in liver (Davis, 2000). We show that mice with compound hepatic ablation of both genes (*Jnk1* and *Jnk2*) exhibit systemic protection against HFD-induced insulin resistance. Moreover, we demonstrate that the peroxisome

proliferator-activated receptor α (PPARα)-fibroblast growth factor 21 (FGF21) hormone axis contributes to metabolic regulation by hepatic JNK.

RESULTS

Establishment of Mice with JNK Deficiency in the Liver

To test the role of hepatic JNK, we compared control mice (L^{WT}) and mice with hepatocyte-specific deficiency of JNK1 ($L^{\Delta1}$), JNK2 ($L^{\Delta2}$), or JNK1 plus JNK2 ($L^{\Delta1,2}$) (Figures 1A and 1B). HFD-induced JNK activation in the liver of L^{WT} mice was partially suppressed in $L^{\Delta1}$ and $L^{\Delta2}$ mice (Figure 1C). In contrast, hepatic JNK activity was not detected in $L^{\Delta1,2}$ mice (Figure 1C). These data indicate that JNK1 and JNK2 may serve partially redundant functions in the liver and confirm the absence of hepatic JNK activity in $L^{\Delta1,2}$ mice. We employed these mouse strains in order to examine the metabolic consequences of hepatic JNK deficiency.

Hepatic JNK Deficiency Reduces Diet-Induced Obesity

We found that hepatic JNK deficiency caused no change in body mass when mice were fed a chow diet (Figure 1D; Figures S1A and S1B available online). Similarly, HFD-fed L^{WT} mice and $L^{\Delta1}$ mice developed equal obesity (Figures 1D, S1A, and S1B). In contrast, HFD-fed $L^{\Delta2}$ mice and $L^{\Delta1,2}$ mice gained less fat mass than HFD-fed L^{WT} mice (Figures 1D, S1A, and S1B). These data indicate that JNK2 deficiency, rather than JNK1 deficiency, most closely mimics the phenotype of compound deficiency of JNK1 plus JNK2.

The reduced obesity of $L^{\Delta1,2}$ mice in comparison to L^{WT} mice was associated with reduced adipose tissue mass (Figure S1B), reduced VLDL triglyceride in serum (Figures S1D and S1E), reduced total serum triglyceride (31.7 ± 0.03 mg/dl in comparison to 64.8 ± 0.09 mg/dl; mean ± SEM; n = 8; $p < 0.03$), reduced hepatic expression of lipogenic genes, including *Srebf1* and *Fasn* (Figures S1F and S1G), and reduced de novo hepatic lipogenesis (Figure S1H). Altogether, these data demonstrate that hepatic JNK deficiency causes dysregulated lipid metabolism.

Hepatic JNK Deficiency Increases Insulin Sensitivity

The HFD-fed $L^{\Delta1,2}$ mice showed improved tolerance to glucose, insulin, and pyruvate (Figures 1E–1G). Hyperinsulinemic-euglycemic clamp studies demonstrated reduced hepatic glucose production, increased hepatic insulin action, improved whole-body insulin sensitivity (detected by increased glucose infusion rates during the clamps), and increased whole-body glycogen plus lipid synthesis (Figures 1H–1K). These data demonstrate that hepatic JNK deficiency causes protection of mice against HFD-induced insulin resistance.

We performed biochemical studies of insulin signaling by measurement of AKT activation in L^{WT} and $L^{\Delta1,2}$ mice. This analysis demonstrated that $L^{\Delta1,2}$ mice were partially protected against the HFD-induced suppression of insulin-stimulated AKT activation in liver, adipose tissue, and skeletal muscle that was detected in L^{WT} mice (Figures 1L–1N). These data confirm the conclusion that HFD-fed $L^{\Delta1,2}$ mice exhibit a systemic increase in insulin sensitivity in comparison to L^{WT} mice. The increased insulin sensitivity of $L^{\Delta1,2}$ mice correlates with reduced HFD-induced islet hypertrophy, hyperinsulinemia, and suppression of glucose-stimulated insulin secretion (Figures 2A–2D). Moreover, HFD-induced hyperglycemia was significantly suppressed in $L^{\Delta1,2}$ mice compared with L^{WT} mice (Figures 2E–2F).

The improved insulin sensitivity of HFD-fed $L^{\Delta1,2}$ mice contrasts with our previous analysis of $L^{\Delta1}$ mice with liver-specific JNK1 deficiency that exhibit increased insulin resistance compared with L^{WT} mice (Sabio et al., 2009). This analysis suggests that hepatic JNK2 may play a critical role in glycemic regulation. Indeed, HFD-fed $L^{\Delta2}$ mice exhibited increased glucose tolerance, reduced islet hypertrophy, and reduced hyperinsulinemia in comparison to HFD-fed L^{WT} mice (Figures S2A–S2F). The HFD-fed $L^{\Delta2}$ mice also exhibited increased insulin sensitivity in hyperinsulinemic-euglycemic clamp studies (Figures S2G–S2M). Nevertheless, these glycemic phenotypes of $L^{\Delta2}$ mice (Figure S2) are modest in comparison to $L^{\Delta1,2}$ mice (Figures 1 and 2). Altogether, these data indicate that $L^{\Delta1}$ mice and $L^{\Delta2}$ mice exhibit different glycemic phenotypes and that $L^{\Delta2}$ mice, and especially $L^{\Delta1,2}$ mice, show improved control of blood glucose concentration compared with L^{WT} mice.

The mechanism that accounts for the differential effects of hepatic JNK1 and JNK2 deficiency is unclear. Previous studies have established that isoforms of JNK with different protein kinase activities are derived by alternative splicing of primary transcripts of the *Jnk1* and *Jnk2* genes (Davis, 2000). Indeed, JNK substrate specificity is determined by the mutually exclusive inclusion of exons 7a or 7b in *Jnk1* and *Jnk2* mRNA that encode JNK isoforms α and β (Gupta et al., 1996). Analysis of hepatic *Jnk* mRNA demonstrated that the major JNK isoforms in liver correspond to JNK1β and JNK2α (Figure S1C). This pattern of alternative splicing of *Jnk* mRNA may contribute to the differential phenotypes caused by ablation of the hepatic *Jnk1* or *Jnk2* genes.

Hepatic JNK Deficiency Increases Fatty Acid Oxidation

Hepatic gene expression in chow- and HFD-fed mice was examined with RNA sequencing (RNA-seq) analysis (Figures S3A and S3B). JNK deficiency caused increased gene expression in HFD-fed mice (Figures S3C–S3E). Gene Ontology analysis demonstrated that $L^{\Delta1}$ mice and $L^{\Delta2}$ mice were markedly different and that $L^{\Delta2}$ mice resembled $L^{\Delta1,2}$ mice (Figures S3F–S3H). Therefore, differentially regulated genes that contribute to the hepatic phenotype of the JNK-deficient mice were identified by comparing gene expression patterns with the glycemic phenotype of the mice ($L^{\Delta1} < L^{WT} < L^{\Delta2} < L^{\Delta1,2}$). Genes downregulated in $L^{\Delta1}$ mice and upregulated in $L^{\Delta1,2}$ mice to a greater extent than $L^{\Delta2}$ mice in comparison to L^{WT} mice were identified, including *Fgf21* (Figures 3A and 3B). Gene Ontology analysis identified significant ($p_{adj} < 0.001$) association of hepatic JNK1 plus JNK2 deficiency with the PPAR pathway and oxidative metabolism (Figure 3C).

To test whether JNK deficiency increases oxidative metabolism, we investigated mitochondrial oxygen consumption by $L^{\Delta1,2}$ and L^{WT} hepatocytes incubated with different substrates. We found that JNK deficiency caused increased mitochondrial oxygen consumption in the presence of palmitate (Figure 3D). In contrast, mitochondrial oxygen consumption by $L^{\Delta1,2}$ hepatocytes metabolizing glucose or pyruvate/lactate was decreased (Figure 3D). Moreover, glucose production by $L^{\Delta1,2}$ hepatocytes metabolizing lactate and pyruvate was increased in comparison

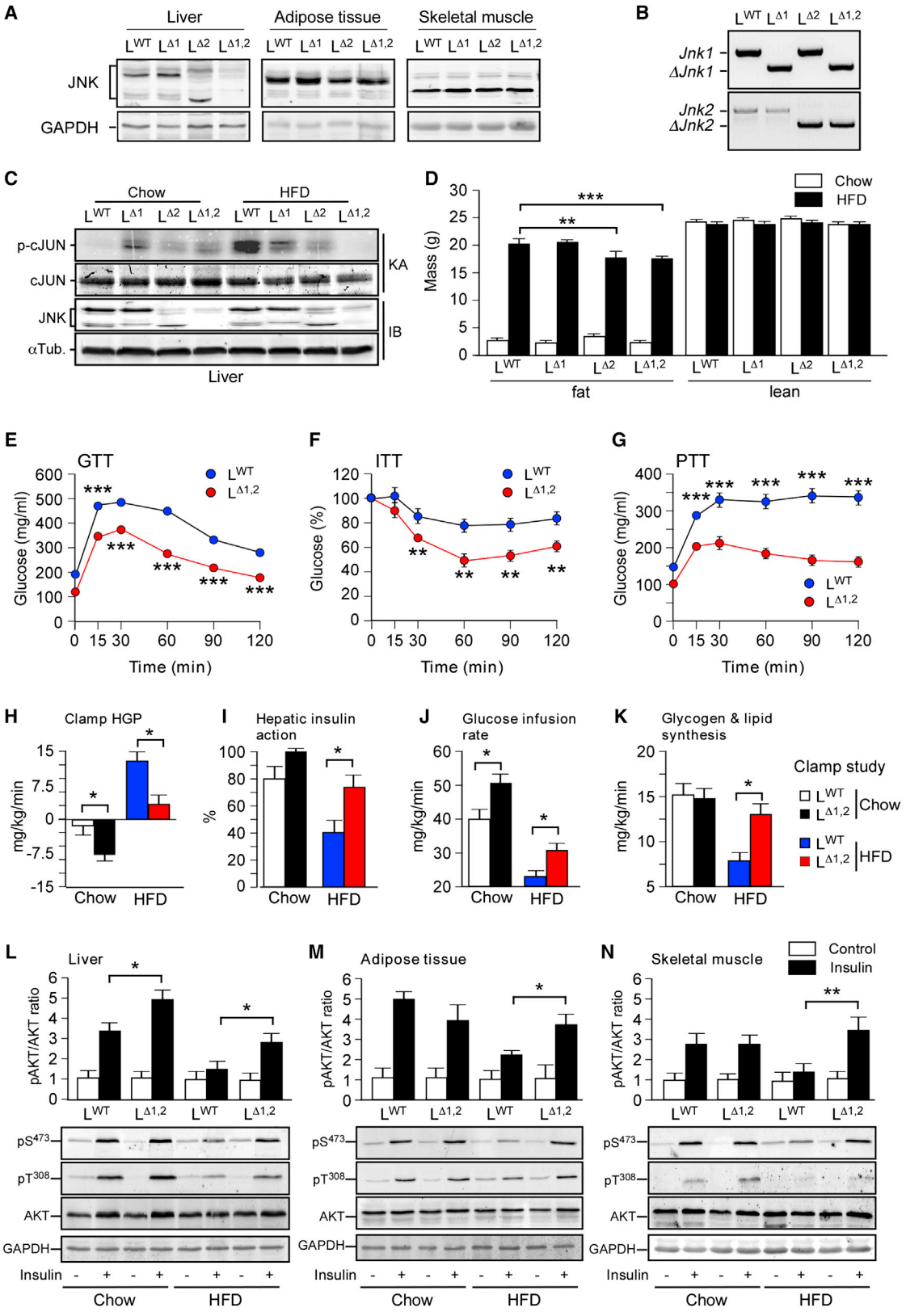

(legend on next page)

to L^{WT} hepatocytes (Figure 3E). This increase in glucose production in vitro was associated with increased expression of the gluconeogenic genes *G6pc* and *Pck1* by $L^{\Delta1,2}$ hepatocytes compared with L^{WT} hepatocytes (Figure S1I). We also found that lactate production by $L^{\Delta1,2}$ hepatocytes metabolizing glucose was increased compared with L^{WT} hepatocytes (Figure 3F). These effects of JNK deficiency were associated with increased expression of citric acid cycle and respiratory chain genes along with increased expression of *Pdk4*, an inhibitor of the oxidative metabolism of pyruvate (Figure 3G). These data demonstrate that JNK deficiency increases the glycolytic conversion of glucose to lactate and selectively promotes the oxidation of fatty acids.

Hepatic JNK Deficiency Activates the PPARα Pathway

The hepatic PPARα pathway (and PPARβ/PPARδ in fat and muscle) increases fatty acid oxidation by peroxisomes, mitochondria, and the endoplasmic reticulum (Evans et al., 2004; Pyper et al., 2010). PPARα pathway activation and increased fatty acid oxidation in the liver of $L^{\Delta1,2}$ mice are reflected by increased PPARα target gene expression (Figure S3B), including genes required for β oxidation in peroxisomes (Figure 3I) and mitochondria (Figure 3J) along with ω oxidation in the endoplasmic reticulum (Figure 3K) in comparison to L^{WT} mice. The $L^{\Delta1,2}$ mice also exhibited increased numbers of hepatic peroxisomes (Figures 4A and 4C), increased mitochondrial size (Figures 4B, 4D, and 4E; consistent with reduced JNK-promoted mitochondrial fission) (Leboucher et al., 2012), and reduced respiratory exchange ratio (Figure S4) in comparison to L^{WT} mice. These data are consistent with the presence of increased PPARα-pathway-stimulated fatty acid oxidation in the liver of $L^{\Delta1,2}$ mice. The increased fatty acid oxidation (Figure 3D), along with reduced lipogenesis (Figures S1F–S1H), contributes to the reduced hepatic steatosis detected in $L^{\Delta1,2}$ mice in comparison to L^{WT} mice (Figure 3H). Because treatment with PPARα agonists can improve glycemia by increasing fatty acid oxidation (Evans et al., 2004; Pyper et al., 2010), PPARα pathway activation may contribute to the phenotype of $L^{\Delta1,2}$ mice (Figures 1 and 2).

The mechanism that mediates PPARα pathway activation in JNK-deficient liver is unclear. Therefore, we examined PPARα-dependent gene expression in primary hepatocytes. Studies of three PPARα target genes (*Acox1*, *Ehhadh*, and *Pdk4*) demonstrated no major differences in the amount of basal expression between $L^{\Delta1,2}$ and L^{WT} hepatocytes. Gene expression was suppressed by treatment with the PPARα antagonists GW6471 or MK886 (Figure 5A). Treatment with the PPARα agonists WY14043 or Fenofibrate caused increased gene expression by L^{WT} hepatocytes that was greatly potentiated in $L^{\Delta1,2}$ hepatocytes (Figure 5A). This increase in PPARα-dependent gene expression was not caused by changes in the expression of PPARα or its heterodimeric partner RXRα (Figure 5B). Reduced expression of corepressors could contribute to increased PPARα function (Perissi et al., 2010; Mottis et al., 2013), and previous studies have established that decreased NCoR1 expression can cause increased nuclear hormone receptor activity (Li et al., 2011; Yamamoto et al., 2011). We found that hepatic JNK deficiency decreased the expression of the PPARα corepressors NCoR1 and NRIP1 (Figures 5B and 5C). The reduced expression of these corepressors may contribute to the metabolic phenotype of $L^{\Delta1,2}$ mice because it is established that reduced expression of NCoR1 (Mottis et al., 2013) or NRIP1 (Nautiyal et al., 2013) is sufficient to promote insulin sensitivity.

To confirm the conclusion that loss of JNK protein kinase activity causes increased PPARα pathway activity, we examined the effect of the selective inhibitor JNK-in-8 (Zhang et al., 2012). This analysis demonstrated that inhibition of JNK protein kinase activity caused increased PPARα target gene expression (*Ehhadh*, *Fgf21*, and *Pdk4*) by primary hepatocytes treated with the PPARα agonist Fenofibrate (Figure 5D). The JNK inhibitor also caused decreased expression of *Ncor1* mRNA (Figure 5D). This observation indicates that the JNK inhibitor and *Jnk* gene ablation cause a similar decrease in *Ncor1* expression and increase in PPARα pathway activity. However, the decrease in *Nrip1* expression detected in $L^{\Delta1,2}$ hepatocytes (Figures 5B and 5C) was not detected when wild-type hepatocytes were treated with the JNK inhibitor (Figure 5D). The mechanism that accounts for this differential regulation of *Nrip1* expression is unclear, but it is possible that short-term pharmacological JNK inhibition may be insufficient to phenocopy the effects of chronic JNK loss-of-function in $L^{\Delta1,2}$ hepatocytes. These data suggest that *Ncor1*, rather than *Nrip1*, represents a key target of hepatic JNK.

Figure 1. Hepatic JNK Contributes to Diet-Induced Obesity and Insulin Resistance

(A) The liver, adipose tissue (epididymal), and skeletal muscle (gastrocnemius) of L^{WT}, $L^{\Delta1}$, $L^{\Delta2}$, and $L^{\Delta1,2}$ mice were examined by immunoblot analysis by probing with antibodies to JNK and GAPDH.

(B) Genomic DNA isolated from the liver of L^{WT}, $L^{\Delta1}$, $L^{\Delta2}$, and $L^{\Delta1,2}$ mice was examined by PCR analysis in order to detect *Jnk* and *ΔJnk* alleles.

(C) Liver extracts prepared from mice fed a chow diet or a HFD (16 weeks) and starved overnight were examined by immunoblot (IB) analysis by probing with antibodies to α-tubulin and JNK. In vitro protein kinase assays (KA) with the substrates GST-cJun and [γ-^{32}P]ATP were performed in order to measure JNK activity. The amount of cJun and phosphorylated cJun (p-cJun) were detected by staining with Coomassie blue and Phosphorimager (Applied Biosystems) analysis, respectively.

(D) The fat and lean mass of chow- and HFD-fed (16 weeks) mice were measured by ^{1}H-MRS analysis (mean ± SEM; n = ~8–10). Significant differences between L^{WT} and $L^{\Delta1,2}$ mice were detected (**p < 0.01, ***p < 0.001).

(E and F) Glucose (GTT) and insulin (ITT) tolerance tests were performed on mice fed HFD (16 weeks; mean ± SEM; n = ~35–50; **p < 0.01; ***p < 0.001).

(G) Pyruvate (PTT) tolerance tests were performed on mice fed HFD (16 weeks; mean ± SEM; n = ~20–30; ***p < 0.001).

(H–K) Insulin sensitivity was measured with hyperinsulinemic-euglycemic clamps with conscious L^{WT} and $L^{\Delta1,2}$ mice fed a chow diet or HFD. The hepatic glucose production (HGP) during the clamp, hepatic insulin action (expressed as insulin-mediated percent suppression of basal HGP), glucose infusion rate, and glycogen plus lipid synthesis (mean ± SEM for ~6–8 experiments) are presented. Statistically significant differences between L^{WT} and $L^{\Delta1,2}$ mice are indicated (*p < 0.05).

(L–N) Chow- or HFD-fed L^{WT} and $L^{\Delta1,2}$ mice were starved overnight and then administered insulin (1.5 U/kg body mass) by intraperitoneal injection. Liver, epididymal adipose tissue, and gastrocnemius muscle extracts (prepared 15 min postinjection) were examined (top) by multiplexed ELISA for pSer^{473}-AKT and AKT (mean ± SEM; n = ~5–6; *p < 0.05). Representative extracts were also examined by immunoblot analysis with antibodies to AKT, phospho-AKT (pSer^{473} and pThr^{308}), and GAPDH (bottom).

See also Figures S1 and S2.

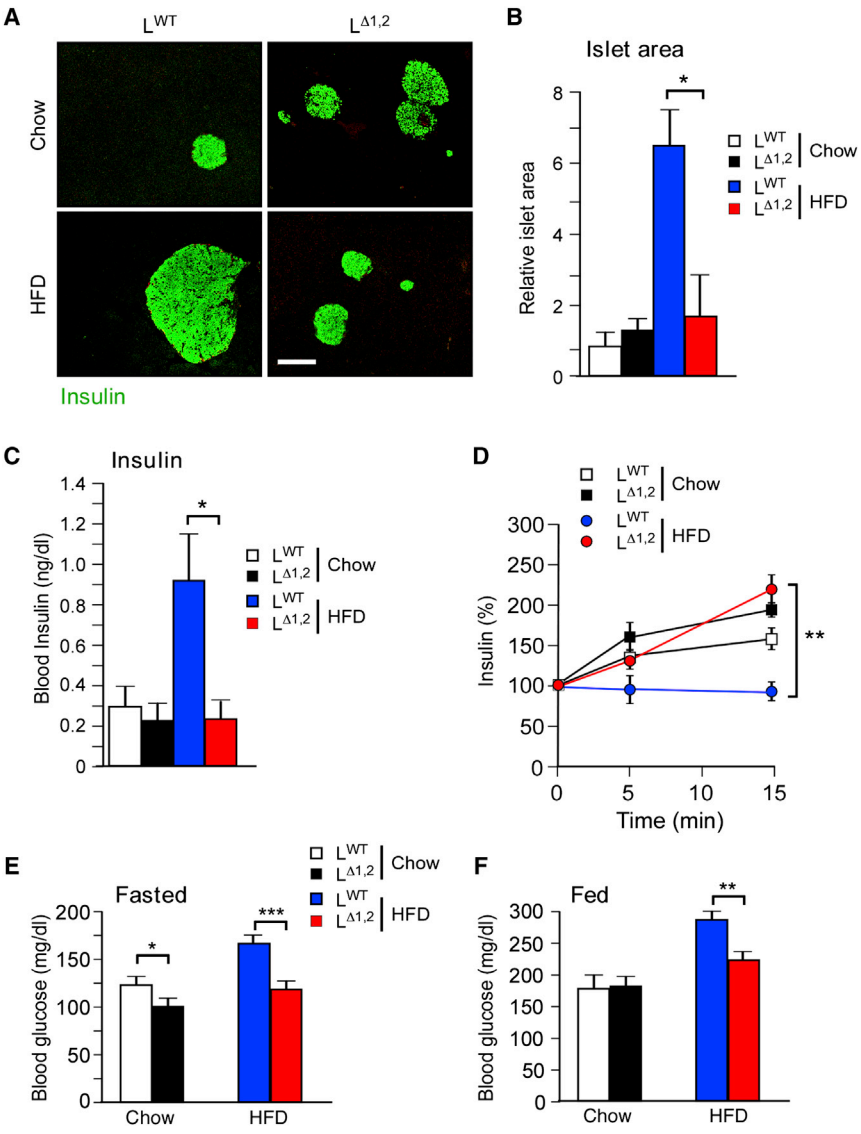

Figure 2. Effect of Liver-Specific JNK Deficiency on Hyperinsulinemia

(A) Mice were fed a chow diet or HFD (16 weeks). Sections of the pancreas were stained with an antibody to insulin. The scale bar represents 100 μm.

(B) Relative islet size was measured with ImageJ (mean ± SEM; n = 30; *p < 0.05).

(C) The mice were fasted overnight, and the blood concentration of insulin was measured (mean ± SEM; n = 16; *p < 0.05).

(D) Glucose-induced insulin secretion was examined using overnight fasted mice by intraperitoneal injection of glucose and measurement of blood insulin concentration (mean ± SEM; n = ~8–10; **p < 0.01).

(E and F) Mice were fed a chow diet or a HFD (16 weeks). Blood glucose concentration in mice fasted overnight or fed ad libitum was measured (mean ± SEM; n = ~35–50; *p < 0.05, **p < 0.01, ***p < 0.001).

To test whether decreased *Ncor1* expression is sufficient to account for PPARα pathway activation, we used small hairpin RNA (shRNA) to knock down hepatic *Ncor1* expression with an adenovirus-associated virus serotype 8 (AAV8) vector. Control studies demonstrated that the AAV8-shNcor1 vector reduced the expression of hepatic *Ncor1* mRNA (Figure 5E). Expression of PPARα target genes (*Fgf21* and *Pdk4*) was increased in the mice treated with the AAV8-shNcor1 vector in comparison to mice treated with the control AAV8-shLuc vector (Figure 5E). These data confirm that reduced NCoR1 expression is sufficient to increase hepatic PPARα pathway activity.

We performed complementation assays to test whether restoration of NCoR1 expression suppressed the effect of hepatic JNK deficiency to increase PPARα target gene expression. Indeed, ectopic NCoR1 expression in the liver of $L^{\Delta1,2}$ mice reduced expression of the PPARα target genes *Acox1*, *Ehhadh*, and *Pdk4* (Figure 5F). Moreover, restoring NCoR1 prevented the effect of JNK deficiency to cause improved glucose tolerance in HFD-fed mice (Figure 5G). Altogether, these data confirm the conclusion that reduced NCoR1 expression contributes to the effects of JNK deficiency on the hepatic PPARα signaling pathway.

A reduction in corepressor expression in JNK-deficient hepatocytes (Figures 5B and 5C) may cause not only increased PPARα activity but also increased activity of other nuclear hormone receptors, including the thyroid hormone receptor that binds NCoR1 (Hörlein et al., 1995). Indeed, reduced NCoR1 expression in the liver caused increased expression of the thyroid hormone receptor target gene *Dio1* (Figure 5E). To test this prediction, we examined triiodothyronine (T3)-stimulated gene expression in primary hepatocytes isolated from L^{WT} and $L^{\Delta1,2}$ mice. We found that JNK deficiency caused significantly increased T3-stimulated expression of thyroid hormone receptor target genes (Figure S5A). Increased expression of these genes in the liver of $L^{\Delta1,2}$ mice in comparison to L^{WT} mice in vivo was detected in the absence of significant changes in the amount of blood thyroid hormone (Figures S5B and S5C). These data support the conclusion that hepatic JNK deficiency may increase the activity of multiple nuclear hormone receptors by decreasing corepressor activity.

Hepatic JNK Deficiency and the PPARγ Pathway

The PPARγ pathway plays an important role in AP1-dependent regulation of hepatic lipid metabolism (Hasenfuss et al., 2014). The mechanism is mediated by increased expression of PPARγ2 that is promoted by cFos heterodimers with cJun/JunB/JunD and is antagonized by Fra1/Fra2 heterodimers with cJun (Hasenfuss et al., 2014). Because AP1 proteins are key targets of the JNK signaling pathway (Davis, 2000), we anticipated that hepatic JNK deficiency may regulate the expression of both AP1 proteins and PPARγ2. Indeed, hepatic

JNK deficiency caused reduced expression of cJun, JunD, Fra2, cFos, and FosB in HFD-fed mice (Figure S6A), but hepatic JNK deficiency caused no significant change in the HFD-induced expression of PPARγ2 (Figure S6B). The absence of a PPARγ2 expression phenotype caused by hepatic JNK deficiency was an unexpected finding that may reflect the balance of positive and negative regulation of PPARγ2 expression by different heterodimeric AP1 transcription factor complexes (Hasenfuss et al., 2014). Nevertheless, compromised hepatic AP1 function in $L^{\Delta1,2}$ mice (Figure S6A) may contribute to decreased expression of *Ncor1* and *Nrip1* (Figures S6C and S6D) and indirectly increase PPARγ pathway activity by reducing corepressor expression.

Hepatic JNK Deficiency Increases Expression of the PPARα Target Gene *Fgf21*

We performed chromatin immunoprecipitation assays in order to examine proteins bound to the promoter of the PPARα target gene *Fgf21* (Figure 6A). This analysis demonstrated that JNK deficiency increased the amount of PPARα bound to the *Fgf21* promoter (Figure 6B). We also found that JNK deficiency reduced the amount of bound NCoR1 (Figure 6C). In contrast, JNK deficiency did not change the interaction of NRIP1 with the *Fgf21* promoter (Figure 6C). As expected, the reduced interaction with NCoR1 was associated with increased histone acetylation on the *Fgf21* promoter (Figure 6D). Altogether, these data indicate that reduced NCoR1 function contributes to increased PPARα pathway activation caused by JNK deficiency in the liver.

The hepatic PPARα pathway plays a major role in ketogenesis (Evans et al., 2004; Pyper et al., 2010). The mechanism is mediated, in part, by PPARα-dependent expression of *Fgf21* (Badman et al., 2007; Inagaki et al., 2007; Badman et al., 2009; Potthoff et al., 2009), a gene that is dysregulated by hepatic JNK deficiency (Figure 3A). Comparison of L^{WT} and $L^{\Delta1,2}$ mice demonstrated that JNK deficiency caused increased hepatic expression of *Fgf21* mRNA (Figure 6E), circulating amounts of FGF21 in the blood (Figure 6F), and ketogenesis (Figure 6G). Complementation assays demonstrated that restoration of hepatic NCoR1 expression (Figure 6H) suppressed the effect of JNK deficiency to cause increased expression of *Fgf21* mRNA in the liver (Figure 6I) and the amount of FGF21 circulating in the blood (Figure 6J). Moreover, shRNA-mediated knockdown of *Ncor1* caused increased hepatic expression of FGF21 (Figure 5E). Altogether, these data confirm that JNK-regulated NCoR1 expression contributes to the effects of JNK to inhibit the PPARα-FGF21 hormone axis.

To test whether increased *Fgf21* expression contributes to the phenotype of $L^{\Delta1,2}$ mice, we used shRNA to knock down hepatic *Fgf21* expression. Control studies demonstrated that an AAV8-shFgf21 vector reduced hepatic *Fgf21* mRNA expression by 75% ± 7% (mean ± SD; n = 6; $p < 0.05$). Moreover, the amount of FGF21 in the blood was reduced in mice treated with the AAV8-shFgf21 vector in comparison to mice treated with the control AAV8-shLuc vector (Figure 7A). We found that the *shFgf21* vector prevented the increased ketogenesis (Figure 7B) and suppressed the improved insulin tolerance (Figure 7C) caused by hepatic JNK deficiency. These data support the conclusion that the PPARα-FGF21 hormone axis contributes to metabolic regulation by hepatic JNK.

FGF21 Contributes to the Systemic Metabolic Effects of Hepatic JNK Deficiency

FGF21 regulates adipose tissue metabolism in part by reducing PPARγ inhibitory sumoylation (Dutchak et al., 2012) and increasing PGC1α expression (Potthoff et al., 2009; Fisher et al., 2012). Therefore, we examined L^{WT} and $L^{\Delta1,2}$ mice to investigate whether hepatic JNK might regulate a FGF21/PPARγ-PGC1α axis in adipose tissue. Analysis of epididymal adipose tissue sections demonstrated that the HFD-induced hypertrophy and macrophage infiltration of L^{WT} adipose tissue were reduced in $L^{\Delta1,2}$ mice (Figure S7A). Gene expression analysis demonstrated decreased expression of macrophage genes, including genes associated with both M1 and M2 polarization, and reduced expression of the adipokine Leptin (Figure S7B). These observations are consistent with the decreased obesity of HFD-fed $L^{\Delta1,2}$ mice in comparison to HFD-fed L^{WT} mice (Figures 1D, S1A, and S1B). We found that $L^{\Delta1,2}$ mice exhibited increased expression of the adipose tissue PPARγ target genes *Adiponectin* (Holland et al., 2013; Lin et al., 2013) and *Fgf21* (Muise et al., 2008; Wang et al., 2008) in comparison to L^{WT} mice (Figure S7B). FGF21-stimulated *Pgc1α* expression has been implicated in the brown-like adaptation of subcutaneous white adipose tissue (Fisher et al., 2012). Indeed, we found increased expression of brown-like genes in the inguinal adipose tissue of HFD-fed $L^{\Delta1,2}$ mice in comparison to HFD-fed L^{WT} mice (Figure S7C). Altogether, these data indicate that FGF21 contributes to the systemic metabolic effects of hepatic JNK deficiency.

DISCUSSION

The liver is a critical organ that orchestrates metabolism within the body. In the fed state, hepatic lipogenesis is increased, and the liver can export triglycerides in the form of very-low-density lipoprotein to peripheral tissues. In contrast, fasting increases hepatic fatty acid oxidation and the delivery of ketone bodies to peripheral tissues. The reprogramming of liver function between these two metabolic states is mediated in part by endocrine hormones (insulin, glucagon, FGF15/FGF19, and FGF21) (Potthoff et al., 2012). The metabolic transition also involves key signal transduction pathways that are differentially activated during feeding and starvation. For example, the PPARα pathway plays an important role during starvation by increasing fatty acid oxidation and ketogenesis and promoting insulin sensitivity (Evans et al., 2004; Pyper et al., 2010). In contrast, the JNK signaling pathway is active in the fed state and is implicated in hepatic steatosis and insulin resistance (Davis, 2000; Sabio and Davis, 2010). These opposing actions of the PPARα and JNK signaling pathways contribute to a metabolic switch that can determine liver function.

This study demonstrates that JNK plays a major role in the regulation of hepatic metabolism by inhibiting nuclear hormone receptor pathways, including PPARα, that increase fatty acid oxidation and ketogenesis. Multiple PPARα target genes likely contribute to these actions of JNK, but *Fgf21* plays a key role in ketogenesis (Badman et al., 2007, 2009), insulin sensitivity (Holland et al., 2013; Lin et al., 2013), glycemia (Kharitonenkov et al., 2005; Xu et al., 2009a, 2009b), and obesity (Kharitonenkov et al., 2005; Coskun et al., 2008). Indeed, suppression of FGF21

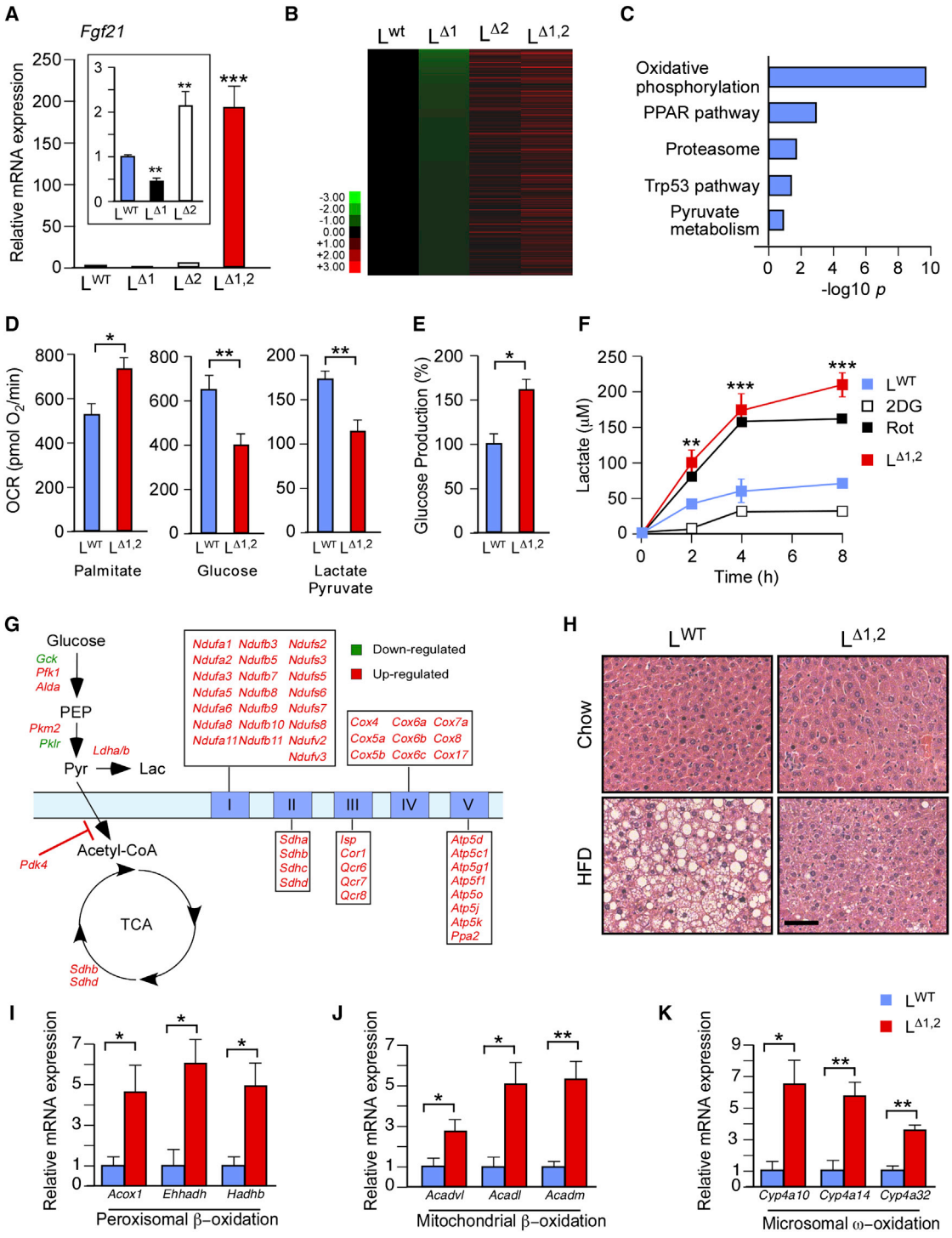

Figure 3. Hepatic JNK Suppresses the PPARα Pathway and Fatty Acid Oxidation

(A) *Fgf21* mRNA expression by primary hepatocytes obtained from L^{WT}, $L^{\Delta1}$, $L^{\Delta2}$, and $L^{\Delta1,2}$ mice was measured by quantitative RT-PCR assays (mean ± SEM; n = 6; **p < 0.01, ***p < 0.001).

(B and C) Heatmap representation of RNA-seq analysis of hepatic genes in overnight fasted HFD-fed mice with the expression profile $L^{\Delta1} < L^{WT} < L^{\Delta2} < L^{\Delta1,2}$. The genes are displayed with lowest expression (top) to highest expression (bottom) in $L^{\Delta1}$ liver. Gene Ontology analysis of these genes is presented (C).

(D–F) Seahorse XF24 analysis was performed using primary hepatocytes isolated from L^{WT} and $L^{\Delta1,2}$ mice. Mitochondrial oxygen consumption rate (OCR) in the presence of 200μM palmitate and BSA, 15 mM glucose, or 1 mM pyruvate and 10 mM lactate (D). Glucose production rate per μg protein in the presence of 1 mM pyruvate and 10 mM lactate (E). Lactate production by L^{WT} and $L^{\Delta1,2}$ hepatocytes (incubated with 15 mM glucose) and the effect of treatment of L^{WT} hepatocytes with 15 mM 2-deoxyglucose (2DG) or 100 nM rotenone (Rot; F). The data presented are the mean ± SEM; n = 10-15; *p < 0.05; **p < 0.01; ***p < 0.001.

(legend continued on next page)

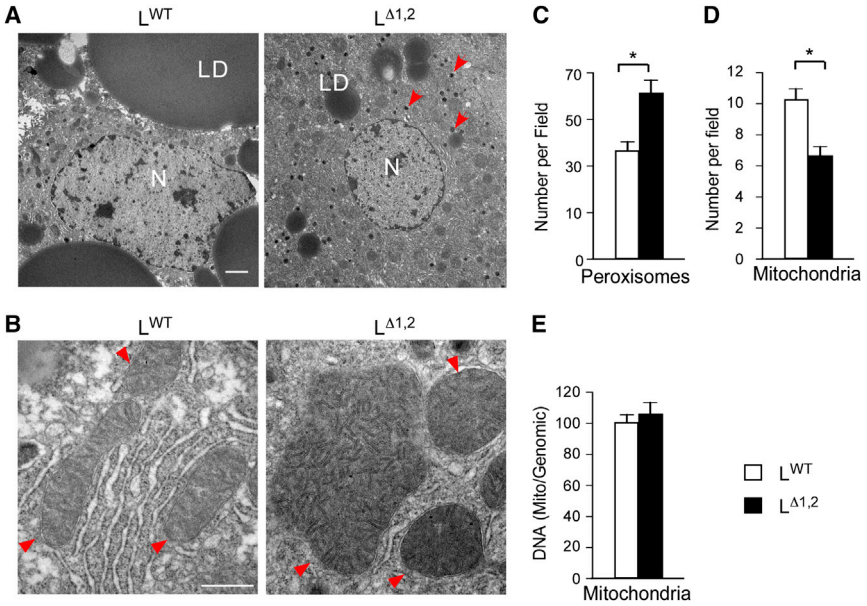

Figure 4. Hepatic JNK Deficiency Increases Peroxisome number and Mitochondrial Size

(A and B) L^{WT} and $L^{\Delta 1,2}$ mice were fed HFD (16 weeks). Sections of the liver were examined by transmission electron microscopy. Representative images are presented. Nucleus, N; lipid droplet, LD. Arrow heads indicate peroxisomes (A) and mitochondria (B).The scale bar represents 2 μm (A) and 0.5 μm (B).

(C and D) The number of peroxisomes (C) and mitochondria (D) per field was measured (mean ± SEM; n = 30; *p < 0.05).

(E) Relative mitochondrial DNA copy number was measured (mean ± SEM; n = 3).

expression in the liver prevents the effects of hepatic JNK deficiency on insulin sensitivity and ketogenesis (Figure 7). Therefore, the PPARα-FGF21 hormone axis is an important target of the hepatic JNK signaling pathway that regulates metabolism.

Our analysis establishes that JNK inhibits PPARα target gene expression in the liver. This effect of JNK is not mediated by changes in the expression of PPARα (or its partner RXRα) but is associated with reduced expression of the corepressors NCoR1 and NRIP1 (Figures 5B and 5C). ChIP assays demonstrated that JNK deficiency changes the interaction of PPARα (increased) and NCoR1 (reduced) with a PPRE in the promoter of the PPARα target gene *Fgf21* (Figures 6A–6C). This reduction in corepressor binding is sufficient to account for PPARα pathway activation (Perissi et al., 2010; Mottis et al., 2013) and may be caused by the reduced corepressor expression detected in mice with hepatic JNK deficiency (Figures 5B and 5C). Indeed, shRNA studies demonstrated that *Ncor1* knockdown was sufficient to cause increased hepatic FGF21 expression (Figure 5E). Moreover, restoration of *Ncor1* expression in the liver prevented PPARα pathway activation (Figure 5F) and FGF21 expression (Figures 6I and 6J) and improved glucose tolerance (Figure 5G) caused by JNK deficiency. These data demonstrate that JNK promotes repression of PPARα target gene expression by regulating corepressor function.

The presence of AP1 sites in the *Ncor1* and *Nrip1* promoters (Figure S6C and S6D) suggests that these genes may be direct targets of a hepatic JNK signaling pathway that activates AP1 (Figure S6A), but other transcription factors or indirect mechanisms (e.g., miRNA pathways) may also contribute to JNK-regulated expression of NCoR1 and NRIP1. Additional analysis will be required to define the mechanism of corepressor regulation by hepatic JNK. Nevertheless, it is established that *Ncor1* mRNA expression is dynamically regulated by exposure of cells to fatty acids and other stimuli that can activate JNK (Yamamoto et al., 2011). Indeed, JNK-stimulated *Ncor1* gene expression may contribute to this dynamic regulation and cause JNK-mediated repression of the PPARα pathway.

Additional studies will be required to test whether PPARα pathway repression is mediated exclusively by JNK-regulated expression of the corepressors NCoR1 and NRIP1. Our analysis does not exclude the possibility that additional factors may contribute to corepressor regulation. Examples include roles for alternative splicing, phosphorylation, nuclear and cytoplasmic transport, protein stability (sumoylation), and protein instability (ubiquitination) (Perissi et al., 2010; Mottis et al., 2013). The possible regulation of NCoR1 degradation by JNK is intriguing because studies of AP1 regulation in macrophages have established that cJun phosphorylation triggers the dissociation and subsequent degradation of NCoR1 (Ogawa et al., 2004). Whether this mechanism is relevant to the PPARα pathway is unclear. Nevertheless, a recent study has highlighted NCoR1 protein turnover as an important regulatory mechanism for gene expression related to energy metabolism (Catic et al., 2013).

The regulation of NCoR1 and NRIP1 expression by JNK suggests that mice with hepatic JNK deficiency may exhibit altered function of multiple nuclear receptors. For example, hepatic NCoR1 functions as a potent inhibitor of thyroid hormone signaling (Feng et al., 2001; Astapova et al., 2008; Fozzatti et al., 2011), and we found that hepatic JNK deficiency caused increased thyroid hormone-dependent gene expression (Figure S5). Similarly, both NCoR1 and NRIP1 inhibit the nuclear

(G) Differentially expressed glycolysis, tricarboxylic acid cycle, and electron transport chain genes identified by RNA-seq analysis in the liver of HFD-fed $L^{\Delta 1,2}$ mice in comparison to HFD-fed L^{WT} are illustrated ($p_{adj} < 0.05$).

(H) L^{WT} and $L^{\Delta 1,2}$ mice were fed a chow diet or a HFD (16 weeks). Sections of the liver were stained with hematoxylin and eosin. The scale bar represents 25 μm.

(I–K) Gene expression in the liver of overnight fasted L^{WT} and $L^{\Delta 1,2}$ mice was measured by quantitative RT-PCR assays of mRNA (mean ± SEM; n = 8; *p < 0.05; **p < 0.01).

See also Figures S3 and S4.

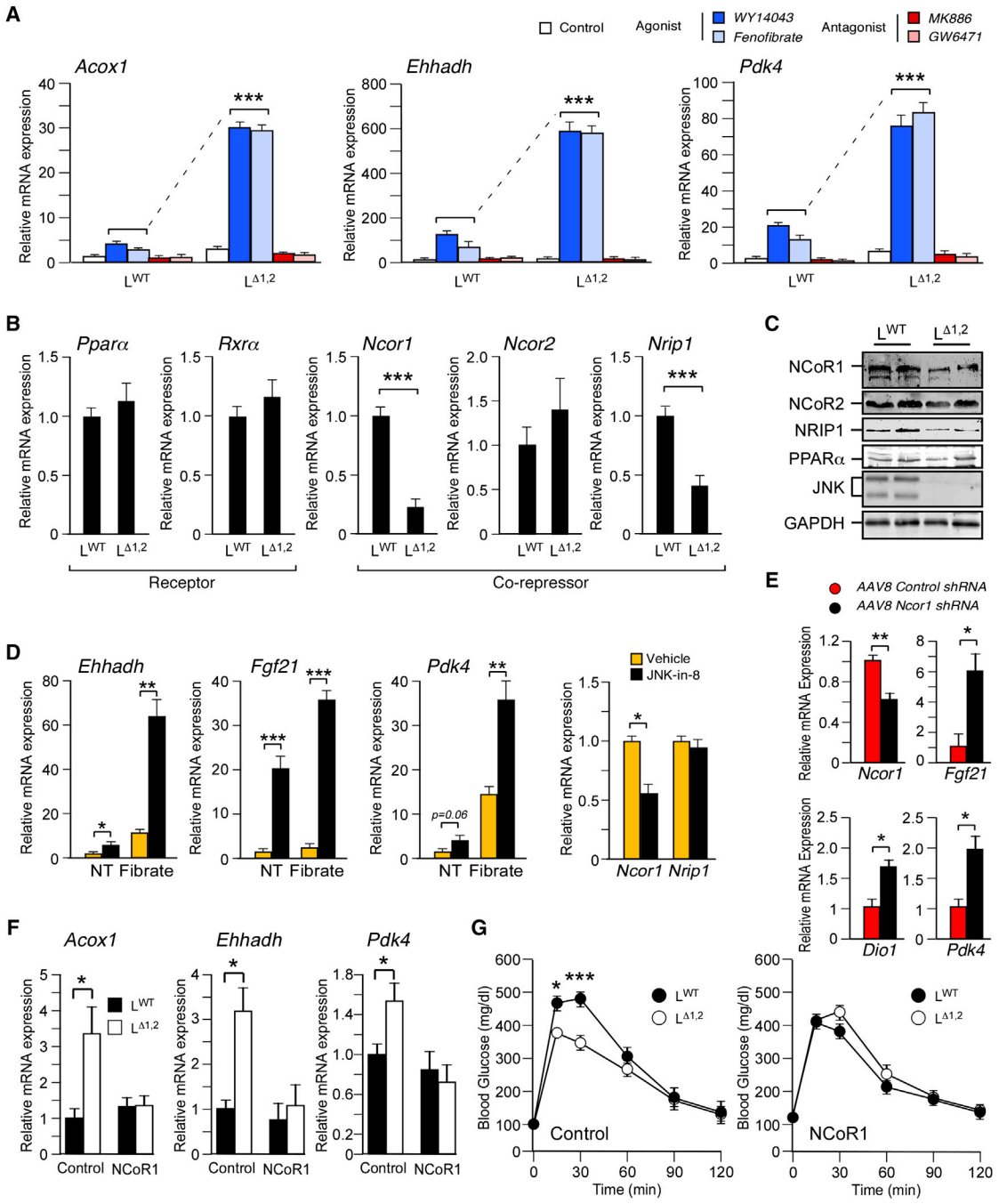

Figure 5. Hepatic JNK inhibits PPARα-Dependent Gene Expression

(A) Primary hepatocytes were obtained from L^{WT} and $L^{\Delta1,2}$ mice and incubated with solvent (DMSO, control), PPARα agonists (50 μM WY14043 or 100 μM Fenofibrate), or PPARα antagonists (10 μM GW6471 or 20 μM MK886) for 16 hr. PPARα target gene (*Acox1*, *Ehhadh*, and *Pdk4*) expression was examined by measurement of mRNA by quantitative RT-PCR analysis (mean ± SEM; n = 6; ***p < 0.001).

(B) The expression of *Pparα*, *Rxrα*, *Ncor1*, *Ncor2*, and *Nrip1* mRNA by L^{WT} and $L^{\Delta1,2}$ primary hepatocytes was measured by quantitative RT-PCR analysis (mean ± SEM; n = 6; ***p < 0.001).

(C) L^{WT} and $L^{\Delta1,2}$ primary hepatocytes were examined by immunoblot analysis by probing with antibodies to PPARα, NCoR1, NCoR2, NRIP1, JNK, and GAPDH.

(D) Primary wild-type hepatocytes were treated (12 hr) with DMSO (vehicle) or 1μM JNK-in-8 (a small molecule JNK inhibitor) prior to measurement of mRNA expression by quantitative RT-PCR analysis (mean ± SEM; n = 6; *p < 0.05, **p < 0.01, ***p < 0.001). The effect of treatment (8 hr) of the hepatocytes with DMSO (NT) or 100 μM Fenofibrate (Fibrate) was examined.

(E) Recombinant AAV8 vectors were employed to express *Control shRNA* or *Ncor1 shRNA* in the liver of HFD-fed (4 weeks) L^{WT} and $L^{\Delta1,2}$ mice. Hepatic mRNA expression at ~10–16 days postinfection was examined by quantitative RT-PCR analysis (mean ± SEM; n = ~14–15; *p < 0.05, **p < 0.01).

(legend continued on next page)

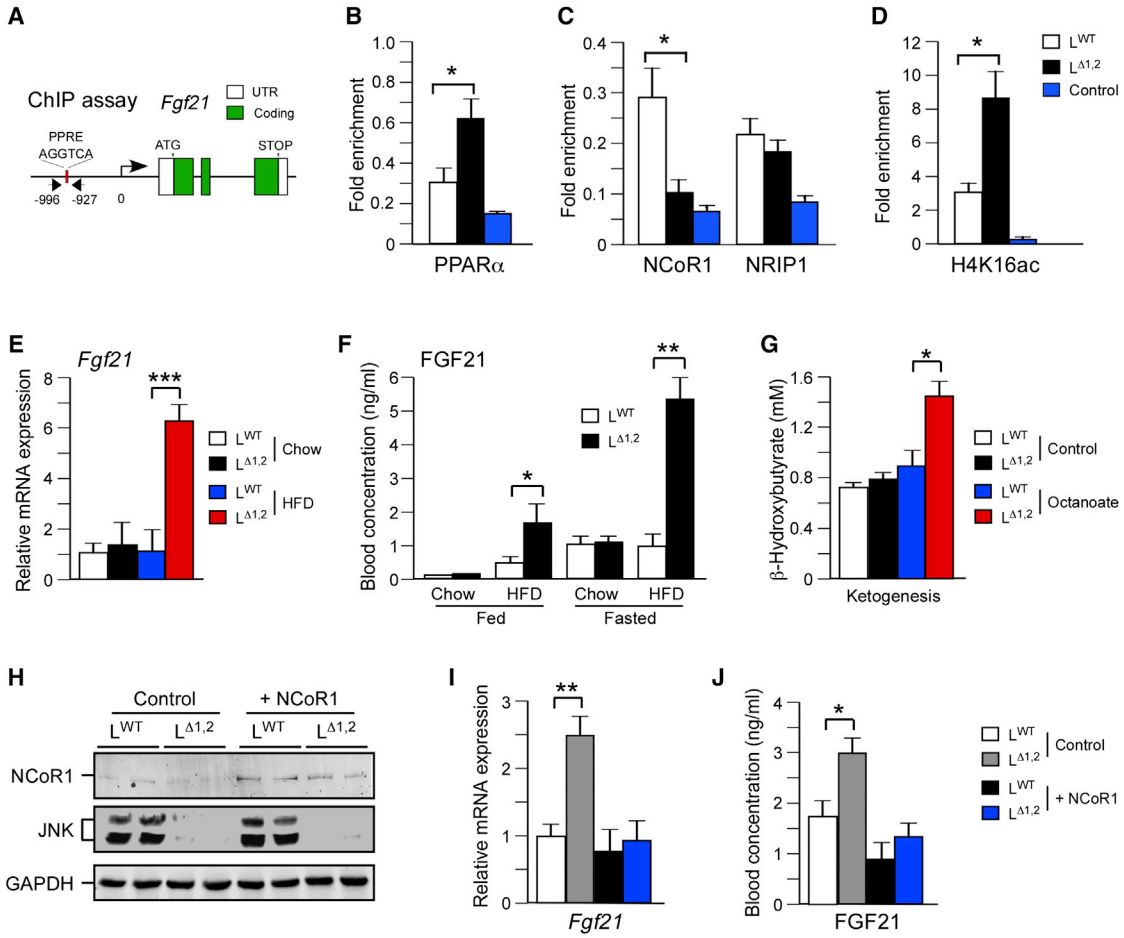

Figure 6. The FGF21 Pathway Is Repressed by JNK

(A–D) Chromatin immunoprecipitation (ChIP) assays were performed with liver isolated from overnight fasted L^{WT} and $L^{\Delta1,2}$ mice with antibodies to nonimmune immunoglobulin (control), PPARα, NCoR1, NRIP1, and acetyl-lysine[16] histone H4 (H4K16ac). The fold enrichment of a fragment of the *Fgf21* promoter with a PPRE site was measured by quantitative PCR analysis (mean ± SEM; n = 6; $p < 0.05$).

(E) The hepatic expression of *Fgf21* mRNA in overnight fasted mice was examined by quantitative RT-PCR analysis (mean ± SEM; n = 8; ***$p < 0.001$).

(F) The concentration of FGF21 in the blood of chow-fed and HFD-fed L^{WT} and $L^{\Delta1,2}$ mice was measured by ELISA. Blood was collected from mice fed ad libitum or fasted overnight (mean ± SEM; n = 6 *$p < 0.05$, **$p < 0.01$).

(G) Ketone body production was measured in overnight fasted L^{WT} and $L^{\Delta1,2}$ mice challenged (6 hr) without (control) and with octanoate (mean ± SEM; n = 5; *$p < 0.05$).

(H–J) NCoR1 or GFP (control) were expressed in the liver of HFD-fed (4 weeks) L^{WT} and $L^{\Delta1,2}$ mice with recombinant adenovirus vectors (~10–16 days). The mice were fasted overnight and hepatic expression of NCoR1 and GAPDH were examined by immunoblot analysis (H). The amount of *Fgf21* mRNA was measured by quantitative RT-PCR analysis (I) and the concentration of FGF21 in the blood was measured by ELISA (J). The data presented are the mean ± SEM; n = 6; *$p < 0.05$, **$p < 0.01$.

See also Figure S7.

hormone receptor liver X receptor (LXR) (Herzog et al., 2007; Astapova et al., 2008). Therefore, JNK deficiency may also regulate LXR, crosstalk with the PPARα pathway (Boergesen et al., 2012), and contribute to the regulation of hepatic lipid metabolism (Beaven et al., 2013). These considerations indicate that there is potential for significant complexity in the hepatic nuclear receptor signaling network that is regulated by JNK. Additional studies will be required to determine the roles of these nuclear receptors (including farnesoid X receptor, glucocorticoid receptor, hepatocyte nuclear factor 4, LXR, and thyroid hormone receptor) in the metabolic response to JNK activation. Nevertheless, our analysis establishes that the PPARα-FGF21 hormone axis is an important mediator of metabolic regulation by hepatic JNK.

(F and G) NCoR1 or GFP (control) were expressed in the liver of HFD-fed (4 weeks) of L^{WT} and $L^{\Delta1,2}$ mice with recombinant adenovirus vectors (~10–16 days). The hepatic expression of *Acox1*, *Ehhadh*, and *Pdk4* mRNA was measured by quantitative RT-PCR analysis (F). The mice were examined by glucose tolerance tests (G). The data presented are the mean ± SEM (n = 6; *$p < 0.05$, ***$p < 0.001$).

See also Figures S5 and S6.

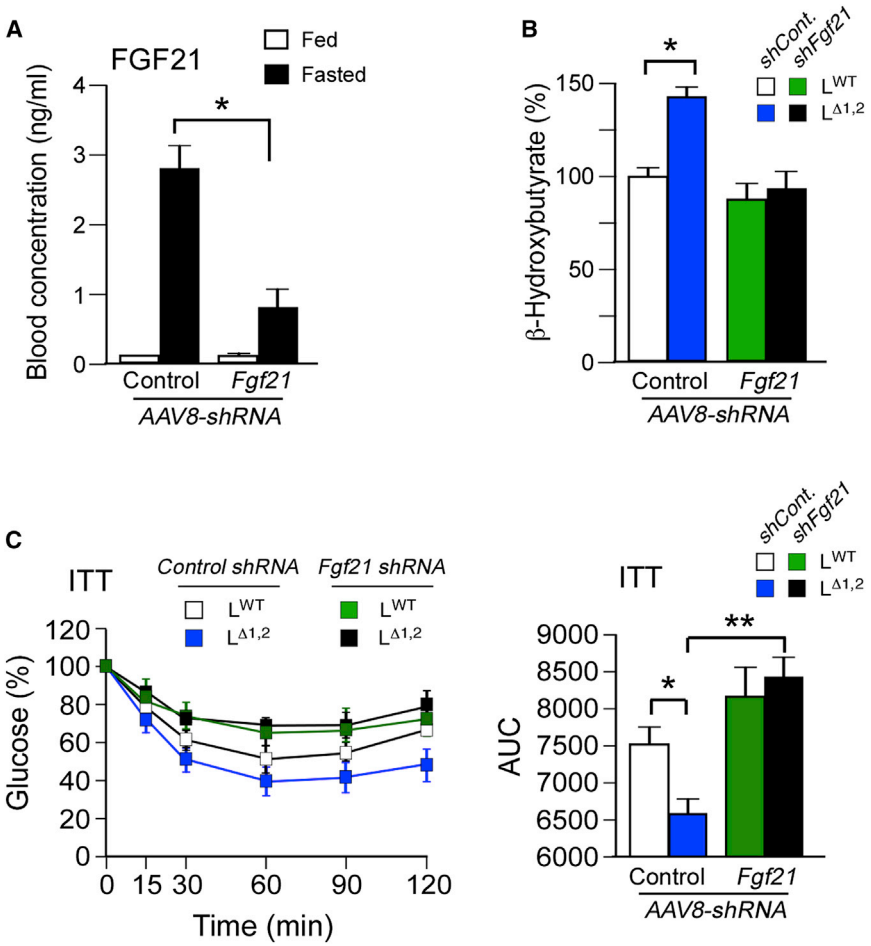

Figure 7. FGF21 Mediates Metabolic Effects of Hepatic JNK Deficiency

(A) AAV8 vectors were employed to express control *shRNA* and *Fgf21 shRNA* in the liver. The mice were fed HFD (4 weeks). FGF21 in the blood of mice fed ad libitum or fasted overnight was measured by ELISA (mean ± SEM; n = 6; *p < 0.05). (B) Ketogenesis was examined in HFD-fed mice that were fasted overnight and then challenged with octanoate (6 hr) by measurement of blood β-hydroxybutyrate (mean ± SEM; n = ~15–30; p < 0.05). The data are normalized to blood β-hydroxybutyrate in control mice at 0 hr (100%). (C) Insulin tolerance tests (ITT) were performed on HFD-fed mice. The time course of blood glucose clearance and the area under the curve (AUC) are presented (mean ± SEM; n = ~15–30; *p < 0.05, **p < 0.01).

Conclusions

The activity of hepatic JNK is regulated by starvation and feeding. These changes in JNK activity regulate the hepatic PPARα-FGF21 hormone axis. Studies of mice with hepatic JNK deficiency demonstrate an exaggerated starvation response (increased ketogenesis) and a reduced response to feeding (protection against hyperglycemia and insulin resistance). These responses are mediated, in part, by the hepatic PPARα-FGF21 hormone axis. Therefore, hepatic JNK plays a key role in diet-mediated metabolic regulation.

EXPERIMENTAL PROCEDURES

Mice

We have previously described Jnk1$^{LoxP/LoxP}$ mice (Das et al., 2007) and Jnk2$^{LoxP/LoxP}$ mice (Han et al., 2013). C57BL/6J mice (stock number 000664) and B6.Cg-Tg(Alb-cre)21Mgn/J mice (stock number 003574) (Postic et al., 1999) were obtained from the Jackson Laboratory. The mice were backcrossed to the C57BL/6J strain (ten generations) and housed in a facility accredited by the American Association for Laboratory Animal Care. The mice employed in this study were L^{WT} (*Cre*$^+$), L^{D1} (*Cre*$^+$ *Jnk1*$^{LoxP/LoxP}$), L^{D2} (*Cre*$^+$ *Jnk2*$^{LoxP/LoxP}$), and L^{D1,2} (*Cre*$^+$ *Jnk1*$^{LoxP/LoxP}$ *Jnk2*$^{LoxP/LoxP}$). All studies were performed with male mice (8–24 weeks old). Male mice (8 weeks old) were fed a standard control (chow) diet or HFD (Iso Pro 3000, Purina, and F3282; Bioserve). Whole-body fat and lean mass were noninvasively measured with ^{1}H-MRS (Echo Medical Systems). The animal studies were approved by the Institutional Animal Care and Use Committee of the University of Massachusetts Medical School.

Viral Transduction Studies

The AAV vector pAAVscCB6siFluc EGFP that expresses an shRNA that targets luciferase was modified by exchanging the luciferase shRNA sequence (*Bam*H1 sites) with a sequence that encodes an *Fgf21* shRNA (5′-GA TCAAAAAAGGGATTCAACACAG GAGAAACTT CGGTTTCTCCTGTGTTGAATCCC-3′). The vector pAAV-RFP-U6 used to express *Ncor1* shRNA (target sequence 5′-CGGCATAATCTT GACAACCTT-3′) was obtained from Vector Biolabs. Recombinant AAV serotype 8 (AAV8) was prepared and amplified by the University of Massachusetts Gene Therapy Vector Core (Mueller et al., 2012; Ahmed et al., 2013). Male mice (8 weeks old) were treated by intravenous injection (tail vein) with 3 × 10^{11} genomic copies per mouse of AAV8-*shLuc* (control), AAV8-*shFgf21*, or AAV8-*shNcor1* (200 μl final volume). Studies were performed ~30–90 days postinfection.

Complementation studies were performed with Ad-GFP (control) and Ad-NcoR1 (NM_001252313) adenovirus stocks obtained from Applied Biological Materials. Male mice (8 weeks old) were fed HFD (4 weeks) and then treated by intravenous injection (tail vein; 200 μl final volume) with 8 × 10^9 genomic copies per mouse of recombinant adenovirus. Studies were performed ~10–16 days postinfection.

Blood Analysis

Blood glucose was measured with an Ascensia Breeze 2 glucometer (Bayer). β-hydroxybutyrate was measured by colorimetric assays (Wako). Insulin and TSH in plasma were measured by multiplexed ELISA with a Luminex 200 machine (Millipore). T3 and T4 (Calbiotech) and FGF21 (Millipore) in plasma were measured with ELISA kits. Serum triglyceride was measured with a kit (Sigma-Aldrich). Lipoprotein analysis was performed by the University of Cincinnati Mouse Metabolic Phenotyping Center.

Glucose, Insulin, and Pyruvate Tolerance Tests

Glucose and insulin tolerance tests were performed by intraperitoneal injection of mice with glucose (1g/kg), insulin (0.5 U/kg), or pyruvate (1g/kg) according to methods described previously (Sabio et al., 2008).

Hepatic Lipogenesis

Mice were starved overnight and refed (3 hr). Lipogenesis was examined in vivo by injecting mice with 20 μCi/g ^3H_2O and measurement of radioactivity incorporation by scintillation counting with adjustments for ^3H_2O-specific activity and tissue mass (Stansbie et al., 1976; Zhang et al., 2006).

Ketogenesis Assays

Ketone body formation in vivo was measured with the ketogenic substrate octanoate (McGarry and Foster, 1971). In brief, mice starved overnight were subjected to intraperitoneal injection of 10 μl/g of 250 mM sodium octanoate in sterile water prior to measurement of β-hydroxybutyrate in the blood (Potthoff et al., 2009).

Hyperinsulinemic-Euglycemic Clamp Studies

The clamp studies were performed by the UMASS Mouse Metabolic Phenotyping Center. After an overnight fast, a 2 hr hyperinsulinemic-euglycemic clamp was conducted in conscious mice with a primed and continuous infusion of human insulin (150 mU/kg body weight priming followed by 2.5 mU/kg/min; Humulin; Eli Lilly), and 20% glucose was infused at variable rates to maintain euglycemia (Kim et al., 2004).

Metabolic Cage Analysis

The analysis was performed by the Mouse Metabolic Phenotyping Center at the University of Massachusetts Medical School. The mice were housed under controlled temperature and lighting with free access to food and water with metabolic cages (TSE Systems).

Statistical Analysis

Differences between groups were examined for statistical significance with a Student's test and ANOVA with the Fisher's test.

ACCESSION NUMBERS

Gene expression data were deposited to the NCBI Gene Expression Omnibus under accession number GSE55190.

SUPPLEMENTAL INFORMATION

Supplemental Information includes Supplemental Experimental Procedures and seven figures and can be found with the article online at http://dx.doi.org/10.1016/j.cmet.2014.06.010.

AUTHOR CONTRIBUTIONS

The study was designed by S.V., G.S., and R.J.D.; experimental analysis was performed by S.V., J.C.-K., L.G-H., and T.B.; metabolic cage and clamp studies were performed by D.Y.J. and J.K.K.; viral vectors were amplified by G.G.; bioinformatic analysis was performed by J.X., H.P.S., and M.G.; and the manuscript was written by S.V. and R.J.D.

ACKNOWLEDGMENTS

We thank Alfredo Giménez-Cassina and Marc Liesa for critical discussions, Shmulik Motola for assistance with RNA-seq analysis, Lara Strittmatter and Greg Hendricks for assistance with electron microscopy, Vicky Benoit for expert technical assistance, and Kathy Gemme for administrative assistance. These studies were supported by a grant from the National Institutes of Health (DK090963). The UMASS Mouse Metabolic Phenotyping Center is supported by grant DK093000. The UMASS Electron Microscopy Core is supported by grants from the National Center for Research Resources (S10RR021043 and S10RR027897). G.S. was supported by the Ramón y Cajal Program and grants ERC 260464, EFSD 2030, MICINN SAF2010-19347, and Comunidad de Madrid S2010/BMD-2326. Centro Nacional de Investigaciones Cardiovasculares is supported by the Ministry of Economy and Competitiveness and the Pro-CNIC Foundation. S.V. was supported by a fellowship from the Ramon Areces Foundation. R.J.D. is an Investigator of the Howard Hughes Medical Institute.

Received: March 3, 2014
Revised: April 30, 2014
Accepted: June 4, 2014
Published: July 17, 2014

REFERENCES

Aguirre, V., Uchida, T., Yenush, L., Davis, R., and White, M.F. (2000). The c-Jun NH(2)-terminal kinase promotes insulin resistance during association with insulin receptor substrate-1 and phosphorylation of Ser(307). J. Biol. Chem. *275*, 9047–9054.

Ahmed, S.S., Li, J., Godwin, J., Gao, G., and Zhong, L. (2013). Gene transfer in the liver using recombinant adeno-associated virus. Curr. Protoc. Microbiol. *Chapter 14*, 6.

Astapova, I., Lee, L.J., Morales, C., Tauber, S., Bilban, M., and Hollenberg, A.N. (2008). The nuclear corepressor, NCoR, regulates thyroid hormone action in vivo. Proc. Natl. Acad. Sci. USA *105*, 19544–19549.

Badman, M.K., Pissios, P., Kennedy, A.R., Koukos, G., Flier, J.S., and Maratos-Flier, E. (2007). Hepatic fibroblast growth factor 21 is regulated by PPARalpha and is a key mediator of hepatic lipid metabolism in ketotic states. Cell Metab. *5*, 426–437.

Badman, M.K., Koester, A., Flier, J.S., Kharitonenkov, A., and Maratos-Flier, E. (2009). Fibroblast growth factor 21-deficient mice demonstrate impaired adaptation to ketosis. Endocrinology *150*, 4931–4940.

Beaven, S.W., Matveyenko, A., Wroblewski, K., Chao, L., Wilpitz, D., Hsu, T.W., Lentz, J., Drew, B., Hevener, A.L., and Tontonoz, P. (2013). Reciprocal regulation of hepatic and adipose lipogenesis by liver X receptors in obesity and insulin resistance. Cell Metab. *18*, 106–117.

Belgardt, B.F., Mauer, J., Wunderlich, F.T., Ernst, M.B., Pal, M., Spohn, G., Brönneke, H.S., Brodesser, S., Hampel, B., Schauss, A.C., and Brüning, J.C. (2010). Hypothalamic and pituitary c-Jun N-terminal kinase 1 signaling coordinately regulates glucose metabolism. Proc. Natl. Acad. Sci. USA *107*, 6028–6033.

Boergesen, M., Pedersen, T.A., Gross, B., van Heeringen, S.J., Hagenbeek, D., Bindesbøll, C., Caron, S., Lalloyer, F., Steffensen, K.R., Nebb, H.I., et al. (2012). Genome-wide profiling of liver X receptor, retinoid X receptor, and peroxisome proliferator-activated receptor α in mouse liver reveals extensive sharing of binding sites. Mol. Cell. Biol. *32*, 852–867.

Catic, A., Suh, C.Y., Hill, C.T., Daheron, L., Henkel, T., Orford, K.W., Dombkowski, D.M., Liu, T., Liu, X.S., and Scadden, D.T. (2013). Genome-wide map of nuclear protein degradation shows NCoR1 turnover as a key to mitochondrial gene regulation. Cell *155*, 1380–1395.

Copps, K.D., Hancer, N.J., Opare-Ado, L., Qiu, W., Walsh, C., and White, M.F. (2010). Irs1 serine 307 promotes insulin sensitivity in mice. Cell Metab. *11*, 84–92.

Coskun, T., Bina, H.A., Schneider, M.A., Dunbar, J.D., Hu, C.C., Chen, Y., Moller, D.E., and Kharitonenkov, A. (2008). Fibroblast growth factor 21 corrects obesity in mice. Endocrinology *149*, 6018–6027.

Das, M., Jiang, F., Sluss, H.K., Zhang, C., Shokat, K.M., Flavell, R.A., and Davis, R.J. (2007). Suppression of p53-dependent senescence by the JNK signal transduction pathway. Proc. Natl. Acad. Sci. USA *104*, 15759–15764.

Davis, R.J. (2000). Signal transduction by the JNK group of MAP kinases. Cell *103*, 239–252.

Dutchak, P.A., Katafuchi, T., Bookout, A.L., Choi, J.H., Yu, R.T., Mangelsdorf, D.J., and Kliewer, S.A. (2012). Fibroblast growth factor-21 regulates PPARγ activity and the antidiabetic actions of thiazolidinediones. Cell *148*, 556–567.

Evans, R.M., Barish, G.D., and Wang, Y.X. (2004). PPARs and the complex journey to obesity. Nat. Med. *10*, 355–361.

Feng, X., Jiang, Y., Meltzer, P., and Yen, P.M. (2001). Transgenic targeting of a dominant negative corepressor to liver blocks basal repression by thyroid hormone receptor and increases cell proliferation. J. Biol. Chem. *276*, 15066–15072.

Fisher, F.M., Kleiner, S., Douris, N., Fox, E.C., Mepani, R.J., Verdeguer, F., Wu, J., Kharitonenkov, A., Flier, J.S., Maratos-Flier, E., and Spiegelman, B.M. (2012). FGF21 regulates PGC-1α and browning of white adipose tissues in adaptive thermogenesis. Genes Dev. *26*, 271–281.

Fozzatti, L., Lu, C., Kim, D.W., Park, J.W., Astapova, I., Gavrilova, O., Willingham, M.C., Hollenberg, A.N., and Cheng, S.Y. (2011). Resistance to

thyroid hormone is modulated in vivo by the nuclear receptor corepressor (NCOR1). Proc. Natl. Acad. Sci. USA *108*, 17462–17467.

Gupta, S., Barrett, T., Whitmarsh, A.J., Cavanagh, J., Sluss, H.K., Dérijard, B., and Davis, R.J. (1996). Selective interaction of JNK protein kinase isoforms with transcription factors. EMBO J. *15*, 2760–2770.

Han, M.S., Jung, D.Y., Morel, C., Lakhani, S.A., Kim, J.K., Flavell, R.A., and Davis, R.J. (2013). JNK expression by macrophages promotes obesity-induced insulin resistance and inflammation. Science *339*, 218–222.

Hasenfuss, S.C., Bakiri, L., Thomsen, M.K., Williams, E.G., Auwerx, J., and Wagner, E.F. (2014). Regulation of steatohepatitis and PPARγ signaling by distinct AP-1 dimers. Cell Metab. *19*, 84–95.

Herzog, B., Hallberg, M., Seth, A., Woods, A., White, R., and Parker, M.G. (2007). The nuclear receptor cofactor, receptor-interacting protein 140, is required for the regulation of hepatic lipid and glucose metabolism by liver X receptor. Mol. Endocrinol. *21*, 2687–2697.

Hirosumi, J., Tuncman, G., Chang, L., Görgün, C.Z., Uysal, K.T., Maeda, K., Karin, M., and Hotamisligil, G.S. (2002). A central role for JNK in obesity and insulin resistance. Nature *420*, 333–336.

Holland, W.L., Adams, A.C., Brozinick, J.T., Bui, H.H., Miyauchi, Y., Kusminski, C.M., Bauer, S.M., Wade, M., Singhal, E., Cheng, C.C., et al. (2013). An FGF21-adiponectin-ceramide axis controls energy expenditure and insulin action in mice. Cell Metab. *17*, 790–797.

Hörlein, A.J., Näär, A.M., Heinzel, T., Torchia, J., Gloss, B., Kurokawa, R., Ryan, A., Kamei, Y., Söderström, M., Glass, C.K., et al. (1995). Ligand-independent repression by the thyroid hormone receptor mediated by a nuclear receptor co-repressor. Nature *377*, 397–404.

Inagaki, T., Dutchak, P., Zhao, G., Ding, X., Gautron, L., Parameswara, V., Li, Y., Goetz, R., Mohammadi, M., Esser, V., et al. (2007). Endocrine regulation of the fasting response by PPARalpha-mediated induction of fibroblast growth factor 21. Cell Metab. *5*, 415–425.

Jaeschke, A., and Davis, R.J. (2007). Metabolic stress signaling mediated by mixed-lineage kinases. Mol. Cell *27*, 498–508.

Kahn, S.E., Hull, R.L., and Utzschneider, K.M. (2006). Mechanisms linking obesity to insulin resistance and type 2 diabetes. Nature *444*, 840–846.

Kant, S., Barrett, T., Vertii, A., Noh, Y.H., Jung, D.Y., Kim, J.K., and Davis, R.J. (2013). Role of the mixed-lineage protein kinase pathway in the metabolic stress response to obesity. Cell Rep *4*, 681–688.

Kharitonenkov, A., Shiyanova, T.L., Koester, A., Ford, A.M., Micanovic, R., Galbreath, E.J., Sandusky, G.E., Hammond, L.J., Moyers, J.S., Owens, R.A., et al. (2005). FGF-21 as a novel metabolic regulator. J. Clin. Invest. *115*, 1627–1635.

Kim, H.J., Higashimori, T., Park, S.Y., Choi, H., Dong, J., Kim, Y.J., Noh, H.L., Cho, Y.R., Cline, G., Kim, Y.B., and Kim, J.K. (2004). Differential effects of interleukin-6 and -10 on skeletal muscle and liver insulin action in vivo. Diabetes *53*, 1060–1067.

Leboucher, G.P., Tsai, Y.C., Yang, M., Shaw, K.C., Zhou, M., Veenstra, T.D., Glickman, M.H., and Weissman, A.M. (2012). Stress-induced phosphorylation and proteasomal degradation of mitofusin 2 facilitates mitochondrial fragmentation and apoptosis. Mol. Cell *47*, 547–557.

Li, P., Fan, W., Xu, J., Lu, M., Yamamoto, H., Auwerx, J., Sears, D.D., Talukdar, S., Oh, D., Chen, A., et al. (2011). Adipocyte NCoR knockout decreases PPARγ phosphorylation and enhances PPARγ activity and insulin sensitivity. Cell *147*, 815–826.

Lin, Z., Tian, H., Lam, K.S., Lin, S., Hoo, R.C., Konishi, M., Itoh, N., Wang, Y., Bornstein, S.R., Xu, A., and Li, X. (2013). Adiponectin mediates the metabolic effects of FGF21 on glucose homeostasis and insulin sensitivity in mice. Cell Metab. *17*, 779–789.

McGarry, J.D., and Foster, D.W. (1971). The regulation of ketogenesis from octanoic acid. The role of the tricarboxylic acid cycle and fatty acid synthesis. J. Biol. Chem. *246*, 1149–1159.

Mottis, A., Mouchiroud, L., and Auwerx, J. (2013). Emerging roles of the corepressors NCoR1 and SMRT in homeostasis. Genes Dev. *27*, 819–835.

Mueller, C., Ratner, D., Zhong, L., Esteves-Sena, M., and Gao, G. (2012). Production and discovery of novel recombinant adeno-associated viral vectors. Curr. Protoc. Microbiol. *Chapter 14*, 1.

Muise, E.S., Azzolina, B., Kuo, D.W., El-Sherbeini, M., Tan, Y., Yuan, X., Mu, J., Thompson, J.R., Berger, J.P., and Wong, K.K. (2008). Adipose fibroblast growth factor 21 is up-regulated by peroxisome proliferator-activated receptor gamma and altered metabolic states. Mol. Pharmacol. *74*, 403–412.

Nautiyal, J., Christian, M., and Parker, M.G. (2013). Distinct functions for RIP140 in development, inflammation, and metabolism. Trends Endocrinol. Metab. *24*, 451–459.

Ogawa, S., Lozach, J., Jepsen, K., Sawka-Verhelle, D., Perissi, V., Sasik, R., Rose, D.W., Johnson, R.S., Rosenfeld, M.G., and Glass, C.K. (2004). A nuclear receptor corepressor transcriptional checkpoint controlling activator protein 1-dependent gene networks required for macrophage activation. Proc. Natl. Acad. Sci. USA *101*, 14461–14466.

Perissi, V., Jepsen, K., Glass, C.K., and Rosenfeld, M.G. (2010). Deconstructing repression: evolving models of corepressor action. Nat. Rev. Genet. *11*, 109–123.

Postic, C., Shiota, M., Niswender, K.D., Jetton, T.L., Chen, Y., Moates, J.M., Shelton, K.D., Lindner, J., Cherrington, A.D., and Magnuson, M.A. (1999). Dual roles for glucokinase in glucose homeostasis as determined by liver and pancreatic beta cell-specific gene knock-outs using Cre recombinase. J. Biol. Chem. *274*, 305–315.

Potthoff, M.J., Inagaki, T., Satapati, S., Ding, X., He, T., Goetz, R., Mohammadi, M., Finck, B.N., Mangelsdorf, D.J., Kliewer, S.A., and Burgess, S.C. (2009). FGF21 induces PGC-1α and regulates carbohydrate and fatty acid metabolism during the adaptive starvation response. Proc. Natl. Acad. Sci. USA *106*, 10853–10858.

Potthoff, M.J., Kliewer, S.A., and Mangelsdorf, D.J. (2012). Endocrine fibroblast growth factors 15/19 and 21: from feast to famine. Genes Dev. *26*, 312–324.

Pyper, S.R., Viswakarma, N., Yu, S., and Reddy, J.K. (2010). PPARalpha: energy combustion, hypolipidemia, inflammation and cancer. Nucl. Recept. Signal. *8*, e002.

Sabio, G., and Davis, R.J. (2010). cJun NH2-terminal kinase 1 (JNK1): roles in metabolic regulation of insulin resistance. Trends Biochem. Sci. *35*, 490–496.

Sabio, G., Das, M., Mora, A., Zhang, Z., Jun, J.Y., Ko, H.J., Barrett, T., Kim, J.K., and Davis, R.J. (2008). A stress signaling pathway in adipose tissue regulates hepatic insulin resistance. Science *322*, 1539–1543.

Sabio, G., Cavanagh-Kyros, J., Ko, H.J., Jung, D.Y., Gray, S., Jun, J.Y., Barrett, T., Mora, A., Kim, J.K., and Davis, R.J. (2009). Prevention of steatosis by hepatic JNK1. Cell Metab. *10*, 491–498.

Sabio, G., Cavanagh-Kyros, J., Barrett, T., Jung, D.Y., Ko, H.J., Ong, H., Morel, C., Mora, A., Reilly, J., Kim, J.K., and Davis, R.J. (2010a). Role of the hypothalamic-pituitary-thyroid axis in metabolic regulation by JNK1. Genes Dev. *24*, 256–264.

Sabio, G., Kennedy, N.J., Cavanagh-Kyros, J., Jung, D.Y., Ko, H.J., Ong, H., Barrett, T., Kim, J.K., and Davis, R.J. (2010b). Role of muscle c-Jun NH2-terminal kinase 1 in obesity-induced insulin resistance. Mol. Cell. Biol. *30*, 106–115.

Stansbie, D., Brownsey, R.W., Crettaz, M., and Denton, R.M. (1976). Acute effects in vivo of anti-insulin serum on rates of fatty acid synthesis and activities of acetyl-coenzyme A carboxylase and pyruvate dehydrogenase in liver and epididymal adipose tissue of fed rats. Biochem. J. *160*, 413–416.

Vernia, S., Cavanagh-Kyros, J., Barrett, T., Jung, D.Y., Kim, J.K., and Davis, R.J. (2013). Diet-induced obesity mediated by the JNK/DIO2 signal transduction pathway. Genes Dev. *27*, 2345–2355.

Wang, H., Qiang, L., and Farmer, S.R. (2008). Identification of a domain within peroxisome proliferator-activated receptor gamma regulating expression of a group of genes containing fibroblast growth factor 21 that are selectively repressed by SIRT1 in adipocytes. Mol. Cell. Biol. *28*, 188–200.

Xu, J., Lloyd, D.J., Hale, C., Stanislaus, S., Chen, M., Sivits, G., Vonderfecht, S., Hecht, R., Li, Y.S., Lindberg, R.A., et al. (2009a). Fibroblast growth factor 21 reverses hepatic steatosis, increases energy expenditure, and improves insulin sensitivity in diet-induced obese mice. Diabetes *58*, 250–259.

Xu, J., Stanislaus, S., Chinookoswong, N., Lau, Y.Y., Hager, T., Patel, J., Ge, H., Weiszmann, J., Lu, S.C., Graham, M., et al. (2009b). Acute glucose-lowering and insulin-sensitizing action of FGF21 in insulin-resistant mouse models—association with liver and adipose tissue effects. Am. J. Physiol. Endocrinol. Metab. *297*, E1105–E1114.

Yamamoto, H., Williams, E.G., Mouchiroud, L., Cantó, C., Fan, W., Downes, M., Héligon, C., Barish, G.D., Desvergne, B., Evans, R.M., et al. (2011). NCoR1 is a conserved physiological modulator of muscle mass and oxidative function. Cell *147*, 827–839.

Zhang, W., Patil, S., Chauhan, B., Guo, S., Powell, D.R., Le, J., Klotsas, A., Matika, R., Xiao, X., Franks, R., et al. (2006). FoxO1 regulates multiple metabolic pathways in the liver: effects on gluconeogenic, glycolytic, and lipogenic gene expression. J. Biol. Chem. *281*, 10105–10117.

Zhang, T., Inesta-Vaquera, F., Niepel, M., Zhang, J., Ficarro, S.B., Machleidt, T., Xie, T., Marto, J.A., Kim, N., Sim, T., et al. (2012). Discovery of potent and selective covalent inhibitors of JNK. Chem. Biol. *19*, 140–154.